Localizing α-Helices in Human Tropoelastin: Assembly of the Elastin "Puzzle" †

ARTICLE *in* BIOCHEMISTRY · SEPTEMBER 2006

Impact Factor: 3.02 · DOI: 10.1021/bi060289i · Source: PubMed

3 AUTHORS, INCLUDING:

Antonietta Pepe
Università degli Studi della Basilicata
67 PUBLICATIONS **887** CITATIONS
SEE PROFILE

Brigida Bochicchio
Università degli Studi della Basilicata
56 PUBLICATIONS **1,052** CITATIONS
SEE PROFILE

Localizing α-Helices in Human Tropoelastin: Assembly of the Elastin "Puzzle"†

Antonio Mario Tamburro,* Antonietta Pepe, and Brigida Bochicchio

Department of Chemistry, Università degli Studi della Basilicata,Via N. Sauro, 85, 85100 Potenza, Italy

Received February 10, 2006; Revised Manuscript Received May 18, 2006

ABSTRACT: Polyalanine cross-linking domains encoded by exons 6, 15, 17, 19, 21, 23, 25, 27, 29, 31 of human tropoelastin were synthesized, and their conformations were studied in different solutions and at different temperatures by CD and ^{1}H NMR. The results demonstrated the presence of poly-proline II helix (PPII) in aqueous solvent and of α-helical conformation in TFE. The ^{1}H NMR results allowed the precise localization of the helices along the peptide sequence. These data were further refined by prediction algorithms in order to take into account the reduced helix stability at the end of the peptides. Furthermore, the influence of flanking residues was checked by synthesizing and by determining the structure of a peptide spanning exon 31 coded domain and the first five residues of the following exon 32 coded domain. These studies, together with those previously published [Tamburro, A. M., Bochicchio, B., and Pepe, A. (2003) *Biochemistry 42,* 13147−62], are used to propose a coherent recomposition of the elastin pieces (domains) in order to give an acceptable solution to the elastin structure−function problem.

Elastin is the protein responsible for the elasticity of vertebrates' tissues such as skin, lung, and large blood vessels, these elastic properties being conferred to it by its assembly in insoluble fibers (*1*, *2*). The elastic properties of elastin have been explained in terms of entropic contribution, and it has also been demonstrated that the basic mechanism is compatible with the classical theory of rubber elasticity (*1*, *3*). An additional goal in elastin research is the revealing of a possible general mechanism of elasticity common to other elastomeric proteins such as spider silk elastic proteins, glutenin, abductin, resilin, etc. (*4*−*6*). Within this context, appreciable results have been obtained for the structure−function relationships of hydrophobic sequences of the soluble precursor protein called tropoelastin (*4*). On the whole, the emerging picture reveals that the conformational features ascertained for the single exon coded polypeptides are the same as those suggested when they are inserted in the entire protein. Therefore, it is possible to use the exon-by-exon analysis to study the role played by a single domain because each exon encodes an independent structure. Circumstantial evidence for that is the finding that some sequences such as those coded by exons 18, 20, and 24 are able to coacervate in a manner similar to the intact tropoelastin molecule. Additionally, other peptides such as that encoded by exons 20 and 30 adopt fibrillar supramolecular structures typical of elastin. Consequently, it is currently possible to know which specific sequences in the parent protein are responsible for specific functions, such as the self-assembly of tropoelastin, and also their contributions to the entropic elasticity. As a result, the approach we used, based on the exon-by-exon synthesis of all polypeptide sequences of human tropoelastin except those pertaining to the polyalanine KA cross-linking domains, was shown to be correct. Nevertheless, further insights are needed for elucidating the structure−function relationships of the polyalanine sequences of elastin and therefore for completing the structural pattern of the protein.

In these regions typically three or two alanine residues separate two lysine residues (*7*−*9*). The lysine residues are responsible for the formation of cross-links important for the elastic mechanical properties. The cross-links are originated by the enzymic oxidation of some lysine ϵ-amino groups which form α-aminoadipic acid δ-semialdehyde (allysine) (*10*). Then, through either aldol condensation or Shiff reactions (dehydro)lysinonorleucine, desmosine, and isodesmosine cross-links are chemically synthesized (*11*−*16*). In order to allow desmosine cross-link formation, the two lysine residues belonging to the same domain have to be positioned at the same side. This structural requirement is perfectly fulfilled in an α-helix structure. Consequently, α-helix conformation was hypothesized to be the structure adopted by the clustering of alanine and lysine residues in the KA domains (*15*).

More recently, the presence of α-helical conformation in elastin was experimentally shown by CD[1] (*17*, *18*) and Raman (*19*) spectra of tropoelastin and by CD of some well-defined recombinant polypeptides spanning the region coded by exons 20 to 24 (*20*); however, it was only supposed to be adopted by the polyalanine sequences.

The first experimental data regarding a desmosine cross-linked peptide isolated from the intact elastin molecule was constituted by a CD spectrum in aqueous solution charac-

† The financial support of EU (QLK6-CT-2001-00332) and MIUR (PRIN2004) is gratefully acknowledged.

* Corresponding author. Tel: ++39 0971 202242. Fax: ++39 0971 202223. E-mail: tamburro@unibas.it.

[1] Abbreviations: CD, circular dichroism; DCC, dicyclohexyl carbodiimide; EX, exon coded peptide; Fmoc, fluorenyl-methoxy-carbonyl; HOBt, hydroxybenzotriazole; MALDI-TOF, matrix assisted laser desorption ionization time-of-flight; NMR, nuclear magnetic resonance; NOE, nuclear Overhauser enhancement; NOESY, NOE spectroscopy; PPII, poly-L-proline II left-handed helix; TFA, trifluoroacetic acid; TFE, 2,2,2-trifluoroethanol; TOCSY, total correlation spectroscopy.

10.1021/bi060289i CCC: $33.50
Published on Web 07/18/2006

teristic of an "extended helix" rather than an α-helix (*16*). The "extended helix" represents the 3_1 left-handed polyproline II helix (PPII), a conformation highly favored in aqueous solution. It has to be noted that both PPII and α-helix conformations allow the lysine residues to lie at a short distance, necessary for condensation of cross-link intermediates (*21*, *22*). In agreement with these data was our finding that a synthetic peptide encoding a KA-type cross-linking region (exon 19 coded domain) is α-helical in aqueous solution (*4*). This was the first case where the results obtained gave precise and detailed information about the exact localization of the helix in the protein. In fact, NMR studies showed the presence of an α-helix spanning the region E6−A15 along the KA sequence.

Within this context, it is known that the lysine residues generally occur in pairs (EX6, EX15, EX21, EX23, EX27, EX29, EX31), but in two instances three lysine residues are found (EX19, EX25). This finding suggested that a given cross-link segment in the formation of a desmosine−isodesmosine serves to join only two tropoelastin molecules rather than four molecules as it is theoretically possible (*23*, *24*). Evidence of that is given by cross-links containing peptides generated by proteolytic digestion of bovine elastin which were studied in order to investigate the alignment of elastin molecules in the mature elastic fiber. In one of these peptides a major cross-linking site in elastin was found. It was formed by the association of sequences encoded by exons 10, 19, and 25. The three chains are joined together by one desmosine and two lysinonorleucine cross-links (*22*, *25*). The authors proposed a structural model where domains 19 and 25 are linked by a desmosine cross-link, while domain 10 (a KP domain) bridges domains 19 and 25 through lysinonorleucine cross-links (*25*). Our group has confirmed this model of interaction. Both a stereochemical mechanism and a possible role for KP sequences were proposed (*26*).

Further evidence for specific protein domain contacts between tropoelastin monomers during association by coacervation and then possibly important for cross-linking was obtained by Weiss and co-workers (*27*). The homobifunctional cross-linker bis(sulfosuccinimidyl) suberate served as a rapid reporter of adjacent lysines and preferentially exposed domains. Intact cross-linked peptide pairs were identified after protease digestion and high-resolution electrospray mass spectrometry followed by MS/MS sequencing. Mapping of the assigned sequences indicated the domains mainly involved in cross-linking. A specificity for particular lysines allowed for the construction of a model for the first close contacts between domains (*27*).

Within this context, we decided to chemically synthesize exon-by-exon all the KA domains on the reasonable assumption that even in this case the conformations adopted by the peptides are the same exhibited by the corresponding sequences in the entire protein. Then NMR, CD data, and several prediction algorithms were used all together to localize the α-helix along the polypeptide sequence. Here, the reductionist approach, previously used for hydrophobic exons (*4*), is a priori allowed because the α-helical structure is strictly sequence dependent and essentially stabilized by short-range interactions. Furthermore, as emphasized above, in at least two cases (*4*, *9*) isolated sequences of elastin have been already demonstrated to maintain the helical conformation. The studies reported in the present paper appear to be fundamental in order to propose a coherent recomposition of the elastin pieces (domains) to give an acceptable solution to the elastin structure.

MATERIALS AND METHODS

Peptide Synthesis and Purification. The peptides were synthesized by using an automatic synthesizer APPLIED BIOSYSTEM model 431 A. Fmoc/DCC/HOBT chemistry was used. The Fmoc-amino acids were purchased from NovaBiochem (Laufelfingen, Switzerland) and from Inbios (Pozzuoli, Italy). The cleavage of peptide from resin was achieved by using an aqueous mixture of 95% trifluoroacetic acid. 1,2-Ethanedithiol, phenol, and thioanisole were also used in the cleavage mixture when necessary. The peptides were lyophilized and purified by semipreparative and preparative reversed-phase high-performance liquid chromatography. Binary gradient was used, and the solvents were H_2O (0.1% TFA) and CH_3CN (0.1% TFA). The purity of peptides was assessed by either electrospray or MALDI-TOF mass spectrometry.

Circular Dichroism. CD spectra of 0.1 mg/mL solutions of peptides were recorded on a Jasco J-600 spectropolarimeter using a HAAKE waterbath as temperature controller using a cell with a path length of 0.1 cm. Usually, 16 scans were acquired in the range 190−250 nm at a temperature of 0 °C, 25 °C, and 60 °C by taking points every 0.1 nm, with a 20 nm min^{-1} scan rate, an integration time of 2 s, and a 1 nm bandwidth. The data were expressed as the molar ellipticity in deg cm^2 $dmol^{-1}$.

Prediction Algorithms. The prediction algorithms used for determining the peptide secondary structure were GOR IV, NNPREDICT, and SSPro and were applied to the entire sequence of human tropoelastin in order to account for possible extension of the helices beyond the limits of the exon-coded sequences. GOR IV is a secondary structure prediction method based on information theory and was developed by J. Garnier, D. Osguthorpe, and B. Robson (*28*−*30*). NNPREDICT is a protein secondary structure prediction algorithm developed at the University of California at San Francisco. Computational neural networks have recently been used to predict the mapping between protein sequence and secondary structure (*31*). SSPro is a secondary structure prediction using bidirectional recurrent neural networks at University of California (*32*).

NMR Studies. All peptides were analyzed by ^{1}H NMR spectroscopy in mixed aqueous/organic solution (TFE-d_3/H_2O 80/20) at 25 °C unless otherwise stated. NMR spectra in aqueous solution were not carried out because CD spectra have established that random coil and/or PPII are present under those conditions. As it is well-known, by NMR it is not straightforward to discriminate between these two conformer populations. The resonance assignment of the ^{1}H NMR spectra was made by standard sequential assignment procedures (*33*) and completed by a combined analysis of 2D-TOCSY (*34*) and 2D-NOESY spectra (*35*) The presence of a considerable number of contiguous alanine residues in the peptide's sequences (up to 10 consecutive alanines, i.e., EX17) made the assignment of the resonance to the different amino acid in the sequence complex. As a result, the narrow chemical shift dispersion of the alanine α-protons caused

Table 1: Sequences of the Cross-Linking Domains of Human Tropoelastin

peptide	sequence	MW (Da)	type
EX6	GLGAFPAVTFPGALVPGGVADAAAAY**K**AA**K**A	2830.2	KA_2K
EX15	GVGPQAAAAAAA**K**AAA**K**F	1570.8	KA_3K
EX17	GVGTPAAAAAAAAAA**K**AA**K**Y	1701.9	KA_2K
EX19	GVVSPEAAA**K**AAA**K**AA**K**Y	1702.9	K_3
EX21	PEAQAAAAA**K**AA**K**Y	1360.5	KA_2K
EX23	GVGTPAAAAA**K**AAA**K**AAQF	1671.9	KA_3K
EX25	GPGGVAAAA**K**SAA**K**VAA**K**AQL	1837.1	K_3
EX27	PGALAAA**K**AA**K**Y	1230.4	KA_2K
EX29	GAGPAAAAAAA**K**AAA**K**AAQF	1684.9	KA_3K
EX31	GIPPAAAA**K**AA**K**Y	1228.4	KA_2K
EX31−32	GIPPAAAA**K**AA**K**YGAAGL	1597.8	KA_2K

severe overlap in the spectra. Nevertheless, almost complete chemical shift assignments and NOE cross-peak analysis was achieved for almost all peptides.

Structure Calculation. Experimental NOE intensities were converted into proton−proton distance constraints classified into three ranges: 1.8−2.7 Å, 1.8−3.3 Å, and 1.8−5.0 Å corresponding, respectively, to strong, medium, and weak NOEs. Pseudoatoms were introduced when no stereospecific assignment was determined, and interproton distances were corrected accordingly (*36*). Structure calculations were run using experimental NOE data collected from NOESY spectra in TFE. The structures were calculated with the CYANA 2.1 program (*37*) using a standard simulated annealing protocol. From an initial ensemble of 100 structures the best 15, in terms of target function values and residual distance restraint violations, were chosen to represent the conformations of the peptides. The resulting structures were analyzed with the MOLMOL graphics program (*38*), which was also used to produce all the molecular plots.

RESULTS

Sequence Analysis. Mainly alanine residues, responsible for α-helical conformation, and lysine residues, responsible for the cross-linking among the polypeptide chains, constitute the KA cross-linking domains. A classification of the ten KA domains present in human tropoelastin sequence is possible considering the number of lysine residues and the spacing between the lysine residues. Two domains (EX19 and EX25) show three lysine residues (K3), and the others show only two lysines, spaced by two (EX6, EX17, EX21, EX27, EX31) (KA_2K) or three alanines (EX15, EX23, EX29) (KA_3K) (Table 1).

Prediction Algorithms. The entire sequence of human tropoelastin (*39*) was submitted to three different secondary structure prediction algorithms: GOR IV, SSpro, and NNpredict. The results were very similar. As a matter of fact, only few differences were found located at the termini of the helices.

The results obtained with the different algorithms were from time to time kept as final results by searching for the best agreement between the different outcomes and are reported in Table 2.

CD Spectroscopy. General Results. The microenvironment that induces the conformation of an amino acid sequence is not known a priori and can be different from the bulk macroscopic solution conditions (i.e., physiological conditions). Predicting the functional solvent environment for insoluble elastin is particularly difficult even if the protein's hydrophobicity and its highly cross-linked nature suggest a less polar internal environment than the surrounding solvent. For this reason, the CD experiments in this study were performed in both water and 2,2,2-trifluoroethanol (TFE) (*4*). TFE is a significantly less polar solvent than water and is usually considered a structure-inducing solvent because it favors intramolecular hydrogen bonding, thus promoting folded conformations such as helices and β-turns (*4*, *40*−*42*). However, are the structures seen under these high concentrations of TFE representative of those in the native protein? It has been shown that "tropoelastin and polypep-

Table 2: Results of Secondary Structure Prediction Algorithms Compared to NMR Results[a]

	Ex6	Ex15
Sequence	GLGAFPAVTFPGALVPGGVADAAAAYKAAKA	GVGPQAAAAAAAKAAAKF
consensus	..................hhhhhhhhhhhh	...hhhhhhhhhhhhhh
NMR	..............ttttthhhhhhhhh..	...hhhhhhhhhhhh..
	Ex17	**Ex19**
Sequence	GVGTPAAAAAAAAAAKAAKY	GVVSPEAAAKAAAKAAKY
consensus	....hhhhhhhhhhhhhh	....hhhhhhhhhhh.
NMR	ttttthhhhhhhhhhhh..	...tthhhhhhhhhh..
	Ex21	**Ex23**
Sequence	PEAQAAAAAKAAKY	GVGTPAAAAAKAAAKAAQF
consensus	hhhhhhhhhhhhh	....hhhhhhhhhhhh.
NMR	..hhhhhhhhh..	ttttthhhhhhhhhh...
	Ex25	**Ex27**
Sequence	GPGGVAAAAKSAAKVAAKAAQL	VPGALAAAKAAKY
consensus	....hhhhhhhhhhhhhhhhh	..hhhhhhhhh
NMR	ttttthhhhhhhhhhhhh...	...hhhhhhh..
	Ex29	**Ex31**
Sequence	GAGPAAAAAAAKAAAKAAQF	GIPPAAAAKAAKY.....
consensus	...hhhhhhhhhhhhhhhh	...hhhhhhhhh.....
NMR	...hhhhhhhhhhhh...	....hhhhhh.....
		Ex31-32
Sequence		GIPPAAAAKAAKYGAAGL
consensus		...hhhhhhhhh....
NMR		....hhhhhhhh.....

[a] h, helix; t, turn.

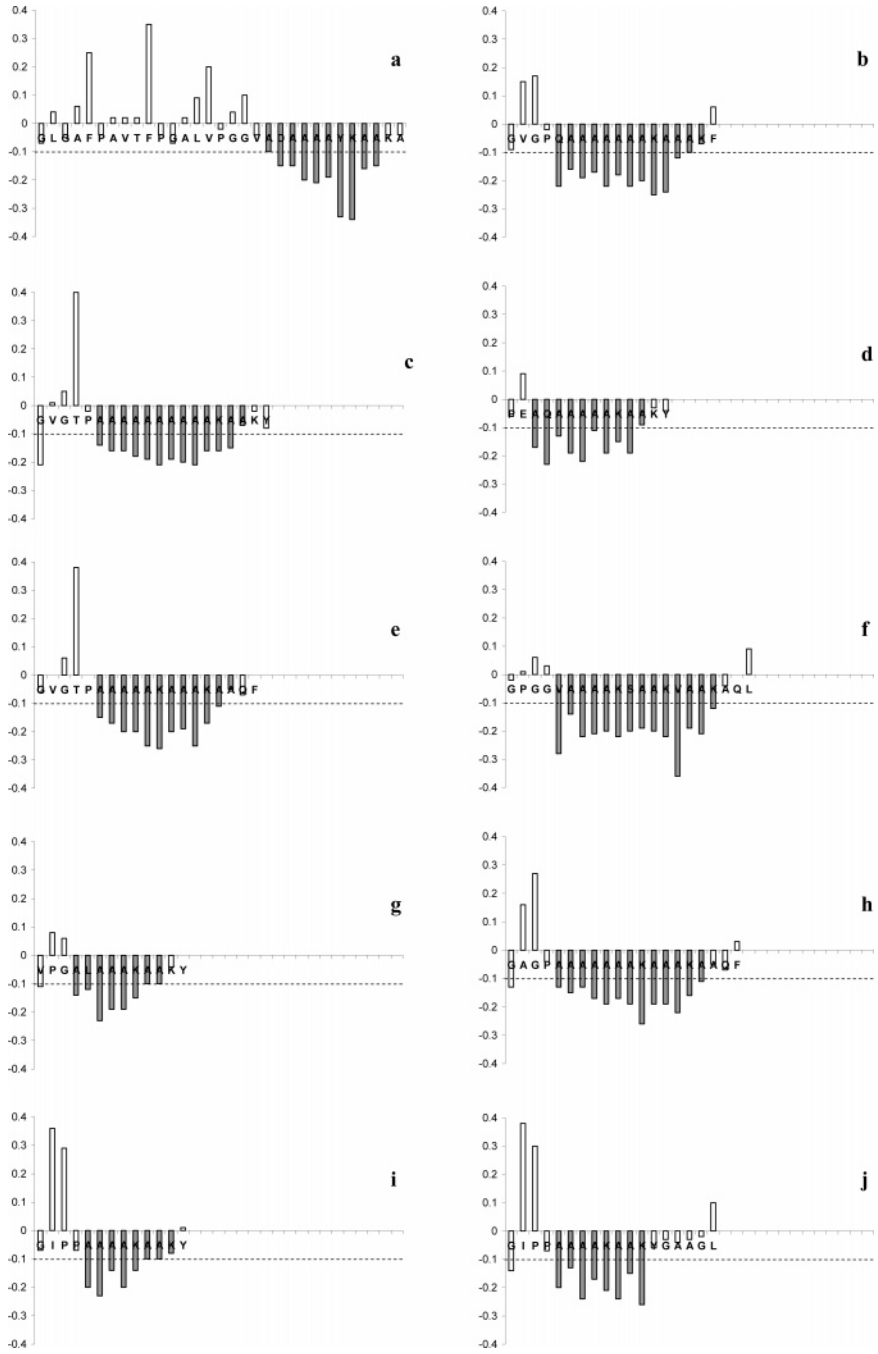

FIGURE 1: CSI of Hα protons of the KA cross-linking domains: (a) EX6; (b) EX15; (c) EX17; (d) EX21; (e) EX23; (f) EX25; (g) EX27; (h) EX29; (i) EX31; (j) EX31−32. Bars in gray refer to α-helical residues.

tides derived from tropoelastin sequences give rise to an organized self-assembly that aligns lysine residues for cross-linking into polymeric structures having the properties of native elastin. This organized self-assembly appears to require a process of hydrophobically driven, temperature-induced phase separation or coacervation, during which a polypeptide rich second phase separates from the bulk solution on elevation of the solution temperature" (*20*). Then, during the coacervation process the microenvironment is highly hydrophobic. Therefore, we suggest that paradoxically TFE mimics better than water the "in vivo" process because it is less polar than water. Furthermore, the use of TFE is a well-established approach to the revealing of α-helical propensity of short peptides. As a matter of fact, they are usually not α-helical in aqueous environment (presumably because of strong hydrogen-bonding interactions with waters), nevertheless expressing their full propensity toward α-helical structure in TFE. The first (but not only one), however still impressive example, is represented by the S-peptide of RNase. This 20 amino acid peptide was found to be essentially unordered in water and 50% helical in TFE (*43*, *44*), a helical percentage identical to that found by X-ray (*45*) in the entire protein. Finally, in order to detect possible temperature-induced conformational transitions, useful for understanding the complexity of conformer population, the peptides were monitored by CD spectroscopy at different temperatures. The results obtained for all the KA sequences can be summarized as follows:

(i) In water the sequences mainly adopt flexible conformations such as PPII helix and the so-called random coil.

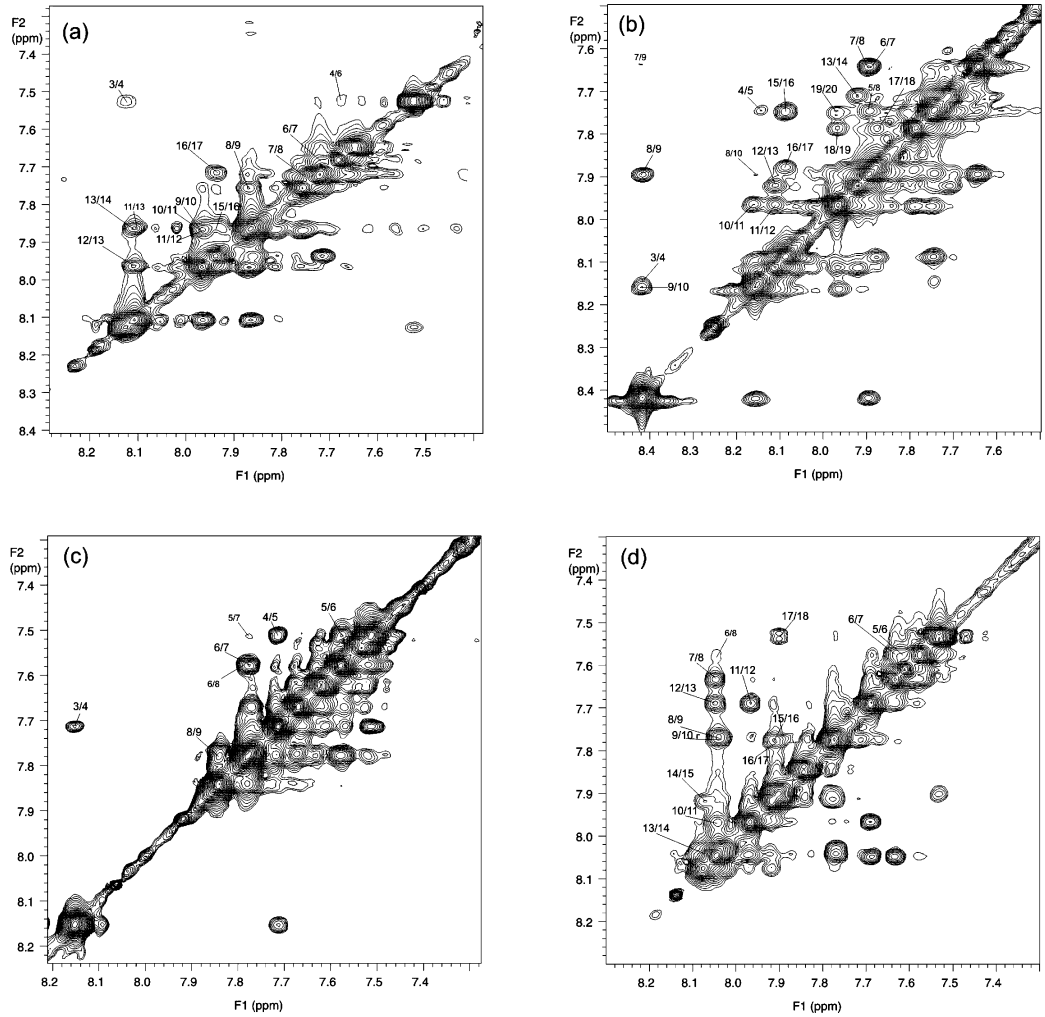

FIGURE 2: Amide region of NOESY spectra of (a) EX23, (b) EX25, (c) EX27, and (d) EX31−32 recorded in TFE-d_3/H_2O (80/20) at 25 °C. Sequential and medium-range d_{NN} NOEs are labeled by residue numbers.

However, the presence of α-helical structures was observed at low temperature for EX17 and in minor amounts for EX15 and EX29, even in the aqueous medium.

(ii) In TFE all the KA sequences take up α-helical conformations shown to be sufficiently stable even at high temperatures (see the following results).

To save space, we are reporting in detail only the CD spectra of some representative sequences, that is, those of EX21, EX23, EX25, EX27, and EX31.

NMR Spectroscopy. CSI Analysis. Proton Hα chemical shifts are sensitive to peptide backbone conformation, and the deviation of the chemical shifts from random coil values has been extensively used to deduce secondary structure in peptides and in proteins. The CSI (chemical shift index) analysis (*46*) allowed proposal of the presence of α-helix for all peptides, the chemical shift values of some Hα protons being upfield shifted with respect to the random coil values (Figure 1). The localization of the α-helix along the peptide sequences through CSI analysis evidenced a certain heterogeneity, due to the size of the peptides and the length of the helix stretch.

NOE Analysis and Structure Calculation. Regular secondary structure elements are derived mainly from a qualitative interpretation of NOEs and $^3J_{\alpha H-NH}$ coupling constants. For all the KA peptides, the NOESY spectra revealed various features consistent with the presence of helical structure, such as more intense intraresidue $d_{\alpha N}(i,i)$ NOEs as compared to sequential $d_{\alpha N}(i,i+1)$.

A systematic search of all the NOE cross peaks typical of helix structure was performed for all the peptides. Figure 2 shows the NOESY amide regions of some representative peptides (EX23) (a), EX25 (b), EX27 (c), EX31−32 (d). In this figure the intense sequential d_{NN} NOEs are indicated, as well as some $d_{NN}(i,i+2)$ NOEs typical for helix structures. Other characteristic NOEs for helical structures are the $d_{\alpha\beta}(i,i+3)$ NOEs and the $d_{\alpha N}(i,i+3)$ present in the NOESY spectra.

A detailed conformational analysis (CD and NMR spectroscopy) will be presented for some representative peptides, that is EX21 and EX27 (KA_2K-type), EX23 (KA_3K-type), and EX25 (K_3-type). Furthermore, the possible end-effect on the stability and localization of the helix has been evaluated by analyzing EX31 and a C-terminal elongated peptide (EX31−32).

EX21. EX21 peptide belongs to the KA_2K-type and is constituted by 14 amino acid residues.

The CD spectra of EX21 in aqueous solution are shown in Figure 3. The spectrum at 0 °C is characterized by a small positive band at about 217 nm and by a strong negative one at about 195 nm. This spectrum is diagnostic of an extended PPII helix (*47*). The presence of PPII is confirmed by the gradual lowering of the band centered at 217 nm and by the

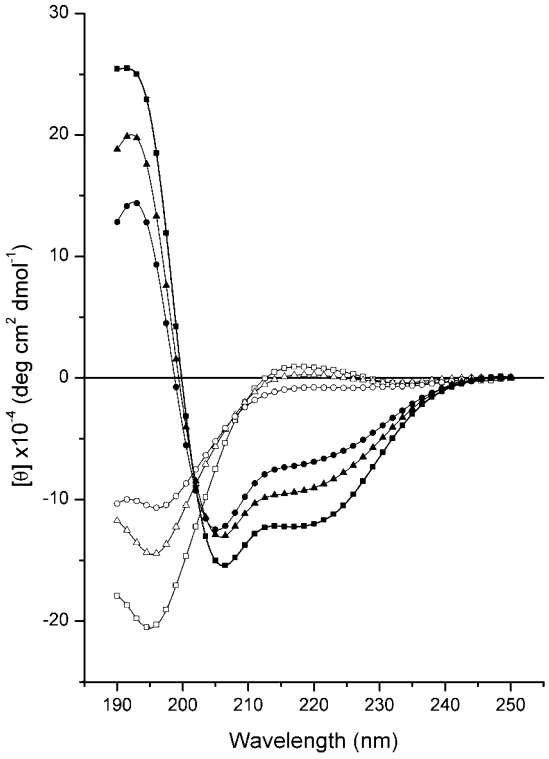

FIGURE 3: CD spectra of EX21 in aqueous solution (empty symbols) and in TFE (filled symbols) recorded at different temperatures: (squares) 0 °C, (triangles) 25 °C, and (circles) 60 °C.

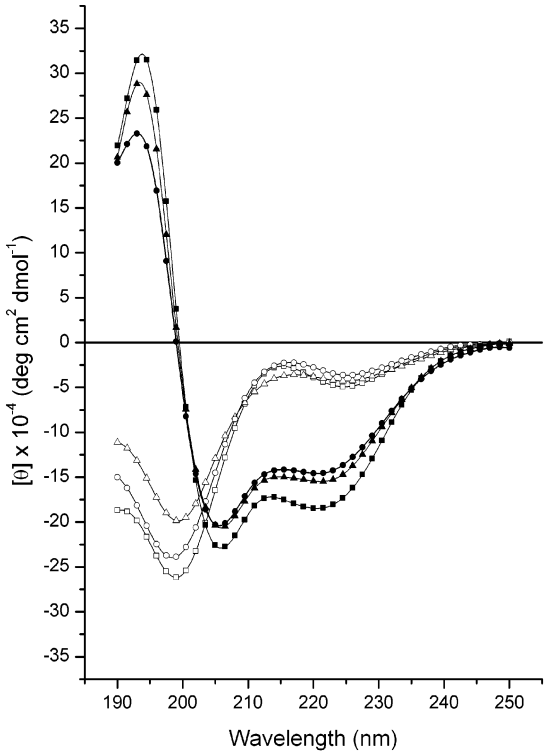

FIGURE 4: CD spectra of EX23 in aqueous solution (empty symbols) and in TFE (filled symbols) recorded at different temperatures: (squares) 0 °C, (triangles) 25 °C, and (circles) 60 °C.

diminishing of the negative one on increasing the temperature to 25 °C and to 60 °C progressively. The conformational features change completely in fluorinated alcohol solution (Figure 3).

In particular, the spectrum at 0 °C shows two small negative bands at 221 nm and at 206 nm and a large positive band at 190 nm, thus suggesting the presence of an α-helix conformation strongly favored by TFE solutions. It is well-known that the band at 222 nm is originated by the n$-\pi^*$ electronic transition and the others at 206 and 190 nm by the $\pi-\pi^*$ electronic components parallel and perpendicular to the helix axis, respectively (*48*). The increasing of the temperature to 25 °C and 60 °C induces small conformational changes such as the progressive decrease of the bands. However, the whole picture is that of a substantial stability of the helix.

NMR spectra recorded in TFE-d_3/H_2O at 25 °C confirm the presence of α-helix. Preliminary, the CSI analysis suggests a helix structure from residue A^3 to residue A^{12} (Figure 1d). Some $J^3_{HN-H\alpha}$ of nonoverlapping peaks were measured from the 1D ^{1}H NMR spectrum. They showed for residues A^3, Q^4, A^6, and A^7 values <5 Hz compatible with α-helix. For residues K^{13} and Y^{14} values are typical of random coil.

A continuous stretch of strong sequential d_{NN} NOEs from residue 3 to 12 data confirmed this localization. Also few $d_{\alpha\beta}(i,i+3)$ and $d_{\alpha N}(i,i+3)$ were identified. Nevertheless, the high overlap of the Hα and Hβ protons of the consecutive alanine residues limited the number of unambiguous NOE connectivities extracted from the NOESY spectrum. As a matter of fact, the distance constraints were not sufficient for structure calculations.

EX23. EX23 peptide belongs to the KA_3K-type domains, and is constituted by 19 residues.

The CD spectra of EX23 in aqueous solution are reported in Figure 4. At 0 °C, a strong negative band below 200 nm and a small negative one at about 225 nm appear. Moreover, a peak at about 215 nm is present, suggesting a trend toward a positive band typical of PPII structure. The increase of the temperature induces a significant decrease of the strong negative band. This behavior is typical of a random coil in equilibrium with PPII conformation, the equilibrium being strongly suggested by the presence of an isoelliptic point. In TFE (Figure 4), the spectrum at 0 °C is very similar to that discussed for EX21. The presence of two small negative bands at about 222 and 206 nm and a positive one at 195 nm are indicative of the occurrence of an α-helix conformation. Also in this case the increase of the temperature induces some decrease of the bands, especially the positive one.

The presence and localization of the α-helix is demonstrated by NMR data, through CSI analysis (Figure 1e) and NOE analysis (Figure 5). The CSI analysis localized the helix in the region A^6-A^{16}. NOE data analysis further refined the localization. Sequential and medium-range NOE connectivities typical of α-helical conformations were found in the region P^5-A^{16}. Strong sequential d_{NN} NOEs are present from A^6 to A^{16}, as well as some $d_{\alpha\beta}(i,i+3)$ and $d_{\alpha\beta}(i,i+3)$ NOEs. The involvement of P^5 in the medium-range NOEs, typical of helix structure, suggests that this residue represent the starting point of the helix. The sequence, G^1VGT^4, preceding the helical stretch is involved in a β-turn as evidenced by strong d_{NN} between G^3 and T^4, a weak $d_{\alpha N}(i,i+2)$ NOE between V^2 and T^4 and by the low-temperature coefficient determined for T^4 amide proton ($\Delta\delta/\Delta T = -2.9$ ppb/K). These features are all compatible with a turn structure. EX23 did not show any long-range NOE (more than five residues

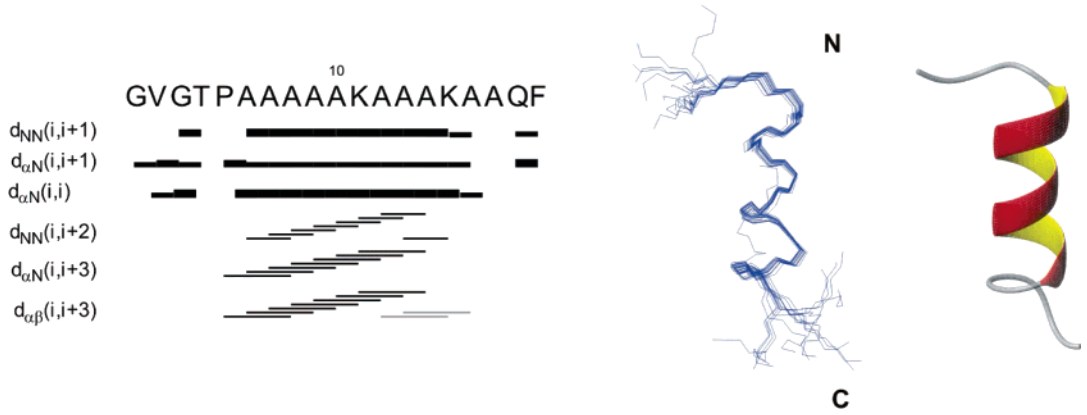

FIGURE 5: NOE summary and calculated structures. (left to right) Summary of intraresidue, sequential, and medium-range NOEs observed for EX23 in 80% TFE-d_3 at 25 °C (the thickness of lines is related to the intensity of NOEs); superposition of the 15 best structures of EX23, best-fitted on residues 2−16 (RMSD: 0.57 ± 0.37 Å on backbone atoms; 1.10 ± 0.36 Å on heavy atoms); ribbon representation of the mean structure of the bundle.

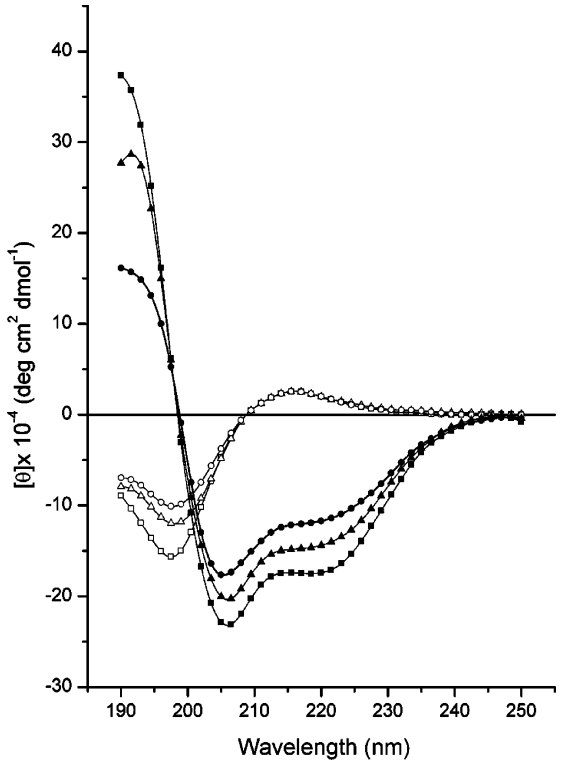

FIGURE 6: CD spectra of EX25 in aqueous solution (empty symbols) and in TFE (filled symbols) recorded at different temperatures: (squares) 0 °C, (triangles) 25 °C, and (circles) 60 °C.

apart). The NOE connectivities together with the chemical shift index obtained for EX23 provided a preliminary localization of the α-helix structure in the region P^5−A^{16}. The NOEs collected in TFE were used as input in CYANA calculations. The 15 best conformers in terms of target function values are shown in Figure 5.

EX25. EX25 peptide belongs to the K_3-type domains and is constituted by 21 residues. At variance with other KA domains, no aromatic residues are present.

The CD spectra of EX25 peptide in aqueous solution (Figure 6) at 0 °C shows a strong negative band below 200 nm, and a small positive one at about 215 nm appears, thus suggesting the presence of PPII structure. The rising of the temperature induces a concomitant decrease of the negative band, a behavior typical of a random coil in equilibrium with PPII conformation, as confirmed by the presence of an isoelliptic point. The spectrum of EX25 in TFE at 0 °C shows a spectral pattern typical of the α-helix conformation (Figure 6) whose amount is decreased by increasing the temperature to 25 °C and to 60 °C.

According to the CSI analysis the helix was localized in the segment V^5−K^{18} (Figure 1f) and also confirmed by NOE data showing series of strong sequential d_{NN} NOEs in the same region. The observation of some medium-range $d_{\alpha\beta}(i,i+3)$ NOEs (G^4/A^7, S^{11}/K^{14}, A^{12}/V^{15}, V^{15}/K^{18}), together with some $d_{\alpha N}(i,i+3)$ (G^4/A^7, A^6/A^9,S^{11}/K^{14}, V^{15}/K^{18}) further confirmed the presence of the α-helix (Figure 7). The NOEs collected in TFE were used as input in CYANA calculations. The 15 best conformers of EX25, in terms of target function values, satisfy well the NOE distance constraints. Figure 7 superimposes the backbone atoms, best fitting residues 5−18, of these 15 best structures of peptide. The peptide presents an α-helical structure from residue 6 to 18, preceded by two type IV β-turns in the region GPGG and GGVA.

EX27. Ex27 belongs to the KA_2K-type cross-link domain and comprises 13 amino acids.

The CD curves (Figure 8) in water clearly indicate the presence of a temperature-dependent PPII structure: on increasing the temperature there is a progressive disappearing of the small positive band at about 217 nm (diagnostic of the PPII structure) and the decreasing of the negative band below 200 nm. Note the presence of an isoelliptic point around 207 nm, demonstrating an equilibrium PPII ⇆ unfolded.

In TFE (Figure 8) the CD spectra are typical of a rather stable α-helix with also a possible type I β-turn (bands at 220, 205, and 193 nm) which are only slightly sensitive to the temperature.

NMR data indicate also for this peptide the presence of a turn preceding the α-helix. The turn was ascertained in the region P^2GAL^5, as pointed out by reduced temperature coefficient of L^5 amide proton ($\Delta\delta/\Delta T = -2.5$ ppb/K) and $d_{\alpha N}(i,i+2)$ NOE connectivity between residue G^3 and L^5.

The CSI analysis suggests that the helix spans the sequence A^4 to A^{11} (Figure 1g). The NOESY spectrum shows the presence of a continuous stretch of strong d_{NN} NOEs for the residues G^3 to A^{11}. Further evidence of the helix structure was given by some $d_{\alpha\beta}(i,i+3)$ for G^3/A^6, L^5/A^8, A^6/K^9, $A^7/$

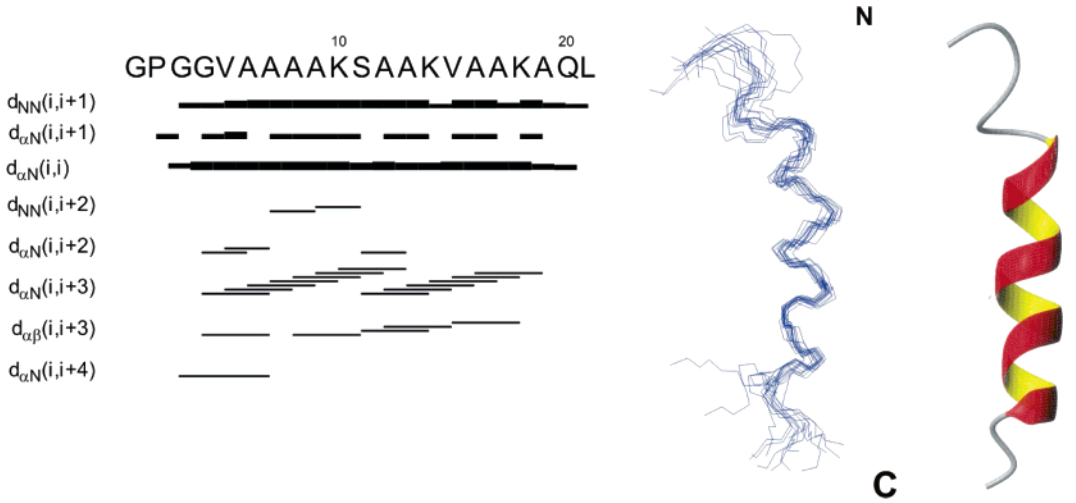

FIGURE 7: NOE summary and calculated structures. (left to right) Summary of intraresidue, sequential, and medium-range NOEs observed for EX25 in 80% TFE at 25 °C (the thickness of lines is related to the intensity of NOEs); superposition of the 15 best structures of EX25, best-fitted on residues 5−18 (RMSD: 1.04 ± 0.38 Å on backbone atoms; 1.66 ± 0.39 Å on heavy atoms); ribbon representation of the mean structure of the bundle.

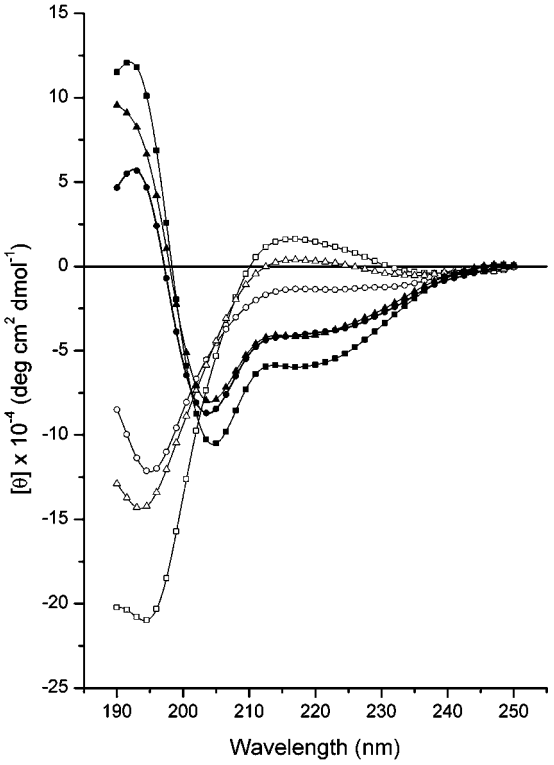

FIGURE 8: CD spectra of EX27 in aqueous solution (a) and in TFE (b) recorded at different temperatures: (squares) 0 °C, (triangles) 25 °C, and (circles) 60 °C.

A^{10}, and A^8/A^{11}, and few $d_{\alpha N}(i,i+3)$ NOEs between G^3/A^6, A^6/K^9, and A^8/A^{11} (Figure 9).

One hundred structures were calculated, and the best 15 conformers in terms of target function values were analyzed by MOLMOL software. The peptide shows a well-defined helical structure from residue 5 to residue 11. The helix is preceded by two turns: a type IV β-turn in the sequence PGAL and a type I β-turn in the region GALA. The Figure 9 superimposes the backbone atoms, best fitting residues 3−11, of these 15 best structures of EX27 peptide.

EX31. EX31 peptide belongs to the KA_2K-type and shows a unique PP sequence preceding the alanine rich region.

The CD spectra of EX31 in aqueous solution are reported in Figure 10. At 0 °C, one strong negative band below 200 nm and a small positive one at about 220 nm appear, thus suggesting the presence of PPII structure. A positive band diagnostic of PPII conformation is usually found at 215 nm which is shifted to 220 nm for peptide sequences rich of proline residues (*49*). The rising of the temperature to 25 °C induces a significant decrease of the negative band although the positive one remains substantially unchanged. This behavior is compatible with the presence of the PPII conformation stable even at room temperature. Only a further increase of the temperature to 60 °C causes the definitive loss of the positive band thus indicating a substantial destabilization of the PPII helix. In TFE the CD spectrum (Figure 10) at 0 °C shows a shoulder at about 222 nm. It also contains a negative band at 204 nm and a positive one at 192 nm at a 1:1 ratio. These conformational features are coherent with the presence of an α-helix coexisting, possibly in equilibrium, in view of the presence of a quasi-isoelliptic point, with an unordered or PPII conformation. The presence of the PPII structure is the preferred interpretation of the spectra because of the noticeable decrease of the negative band at 222 nm most probably caused by the positive ellipticity characteristic of the PPII in that region.

By CSI, the helix is spanning the sequence A^5 to A^{11} (Figure 1i). The NOE analysis shows strong sequential d_{NN} NOEs; also a $d_{NN}(i,i+2)$ between A^8 and A^{10} is evident (Figure 11A).

The structural analysis of the 15 best structures in terms of target function values shows some interesting features. The presence of the two consecutive proline residues confers to the N-terminus an extended PPII-like conformation. The α-helix spans the sequence A^5 to K^{12}, even if in the region A^{10} to A^{12} it has a somewhat irregular form and therefore was not recognized as such by the software that identifies secondary structure implemented in MOLMOL (Figure 11A).

In order to get further support for our approach, to be added to the data previously obtained for the hydrophobic EX5 (*50*), we decided to extend the sequence of EX31 to 5 amino acid residues on the N-terminus of EX32. The obvious aim was to ascertain whether the helix remains of constant

FIGURE 9: NOE summary and calculated structures. (left to right) Summary of intraresidue, sequential, and medium-range NOEs observed for EX27 in 80% TFE at 25 °C (the thickness of lines is related to the intensity of NOEs); superposition of the 15 best structures of EX25, best-fitted on residues 3−11 (RMSD: 0.44 ± 0.26 Å on backbone atoms; 0.91 ± 0.25 Å on heavy atoms); ribbon representation of the mean structure of the bundle.

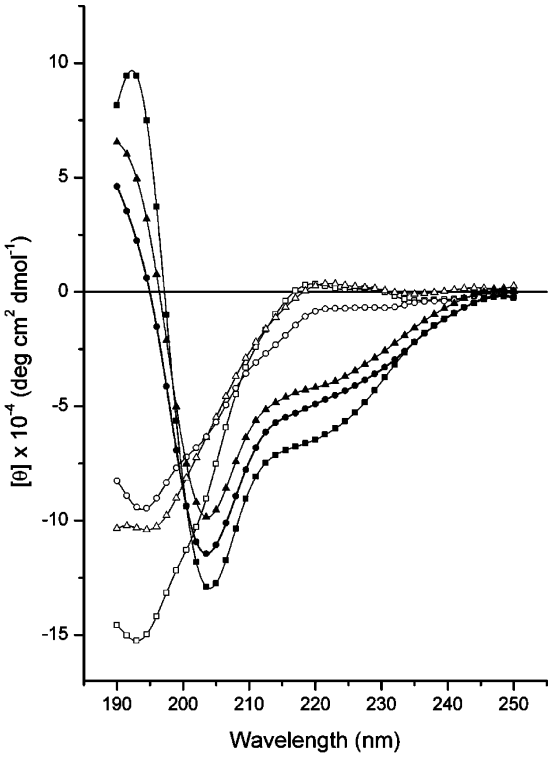

FIGURE 10: CD spectra of EX31 in aqueous solution (empty symbols) and in TFE (filled symbols) recorded at different temperatures: (squares) 0 °C, (triangles) 25 °C, and (circles) 60 °C.

size or it may extend itself to additional residues. As a matter of fact, the corresponding peptide GIPPAAAAKAAKYGAAGL (EX31−32) was studied by NMR.

NMR data of EX31−32 show that the addition of 5 residues to the C-terminus leaves substantially unchanged the helix observed in EX31. In fact, as demonstrated by CSI, the helix is essentially spanning the same number of residues (Figure 1i,j). In fact K^{12} of EX31 exhibits a negative value of CSI even if the classical limit figure of −0.1 is not reached, while the same residue in EX31−32 shows a CSI value more negative. This is most probably due to the presence of the terminal negative charge close to that residue. Some NOE connectivities found for peptide EX31−32 suggest that also Y^{13} could be helical: in any case, the helix increases its size of only 1 residue, always remaining in the region belonging to EX31 domain. Because of better chemical shift dispersion of the amide protons of the C-terminal region, a higher number of NOE derived constraints were extracted from the NOESY spectra (Figure 11B). As a consequence the 15 best conformers of the 100 calculated structures show a minor RMSD in the helical region (Figure 11B). Nevertheless, superposition of the EX31 and EX31−32 mean structures clearly shows that the helices' extent is comparable in the two peptides (Figure 11C). The C-terminal region of EX31−32 peptide, constituted by the 5 residues belonging to exon 32 coded domain, was essentially unordered.

Helix Stability and Helix Propensity. Finally, as comprehensive results, we show in Figure 12a the stability of the helices in TFE as a function of temperature for all studied peptides. The stability of the helix was monitored by the ellipticity at 222 nm $[\theta]_{222}$, a parameter well-known for its sensitivity to the α-helical conformer population. Furthermore, the propensity for assuming α-helical structures for all the sequences studied was determined as a function of TFE percentage (Figure 12b). While the structural stability against temperature is essentially invariant, the propensities are different and in a general sense strongly depend on the number of alanine residues. Lower concentrations of TFE are enough to induce the α-helical conformation for peptides with longer helix stretches.

DISCUSSION

In this Discussion the assumption is made that the helices found by NMR in TFE are essentially those present in the protein under physiological conditions. The rationale is that cross-linking only occurs with coacervation and coacervation rejects water. Parenthetically, this would also promote desmosine condensation because of spatial proximity as already stated in the introduction (*20*, *26*). Thus the α-helical structure, which might only form upon coacervation, should accordingly be a motif present in mature cross-linked elastin. Furthermore, the application of prediction algorithms to the entire protein reveals the presence of α-helical structures in almost the same regions of the protein (Table 2). These findings strength the hypothesis that the α-helices found by us are physiologically relevant.

Now, what can we learn from the localization of α-helices in human tropoelastin?

(i) First of all, the helices appear to be rather stable against temperature, and the amount of periodic structures depends on the number of consecutive alanine residues (EX17, ten

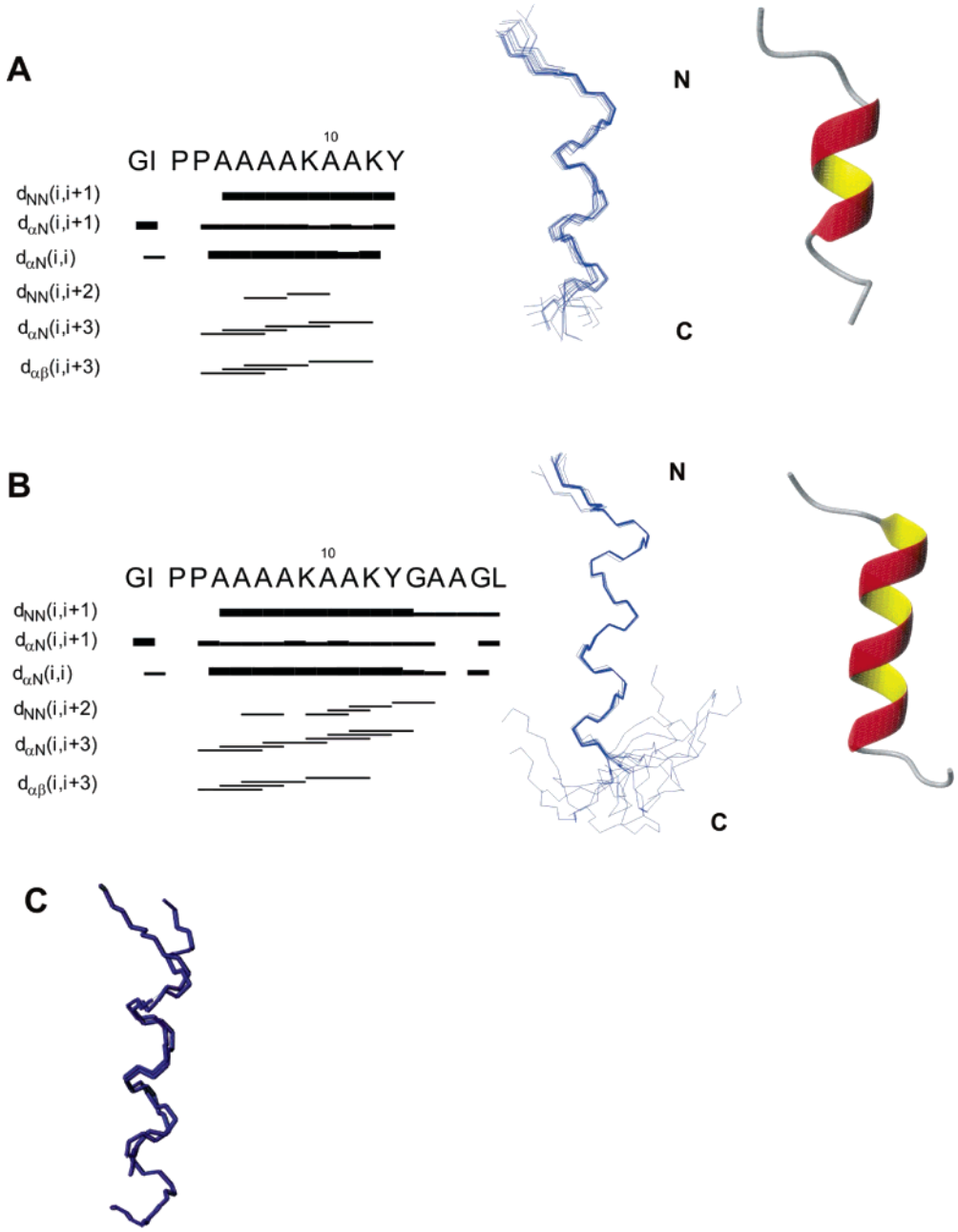

FIGURE 11: NOE summary and calculated structures. (A) (left to right) Summary of intraresidue, sequential, and medium-range NOEs observed for EX31 in 80% TFE-d_3 at 25 °C (the thickness of lines is related to the intensity of NOEs); superposition of the 15 best structures of EX31, best-fitted on residues 3−12 (RMSD: 0.41 ± 0.21 Å on backbone atoms; 0.99 ± 0.26 Å on heavy atoms); ribbon representation of the mean structure of the bundles. (B) (left to right) Summary of intraresidue, sequential, and medium-range NOEs observed for EX31−32 in 80% TFE-d_3 at 25 °C (the thickness of lines is related to the intensity of NOEs); superposition of the 15 best structures of EX31−32, best-fitted on residues 3−13 (RMSD: 0.14 ± 0.10 Å on backbone atoms; 0.71 ± 0.22 Å on heavy atoms); ribbon representation of the mean structure of the bundles. (C) Superposition of the mean structures of EX31 and EX31−32 shows that the extent of the helices is comparable for the two peptides.

alanine residues, and EX15 and EX29, seven alanine residues). In particular, EX29 and EX17 show the presence of α-helix even in aqueous solution at 0 °C. It is assumed that the propensity is inversely proportional to the percentage of TFE necessary to induce the formation of α-helices in mixed solvent. Less propensity is shown by EX6 and EX31 with only four consecutive alanines and by EX21 with five.

(ii) When present (seven out of ten) after the poly-alanine sequence the aromatic residue (Y or F) represents a C-terminal stop signal for the helix. More generally, one can say that no helices appear after the aromatic residues. In fact, when EX31 was prolonged until L^5 residue of the exon 32 coded domain, the helix stopped anyway at the tyrosyl residue. Quite interestingly, there is an almost perfect coherence between the end of the exon-coded sequence and the end of the helix; in all cases, perhaps but one, the prolyl residue represents the N-terminal starting signal for the helix, sometimes being included in an N-terminal β-turn. In particular, at the N-terminus, in seven cases but ten, there are one or two β-turns as stop signals for the α-helices. Quite interestingly, in Exon 19 the β-turn spans the sequence SPEA almost identical to the β-turn SPEL already found in the rarely expressed exon 26A coded domain of human tropoelastin. Also in this case the turn is contiguous to a short

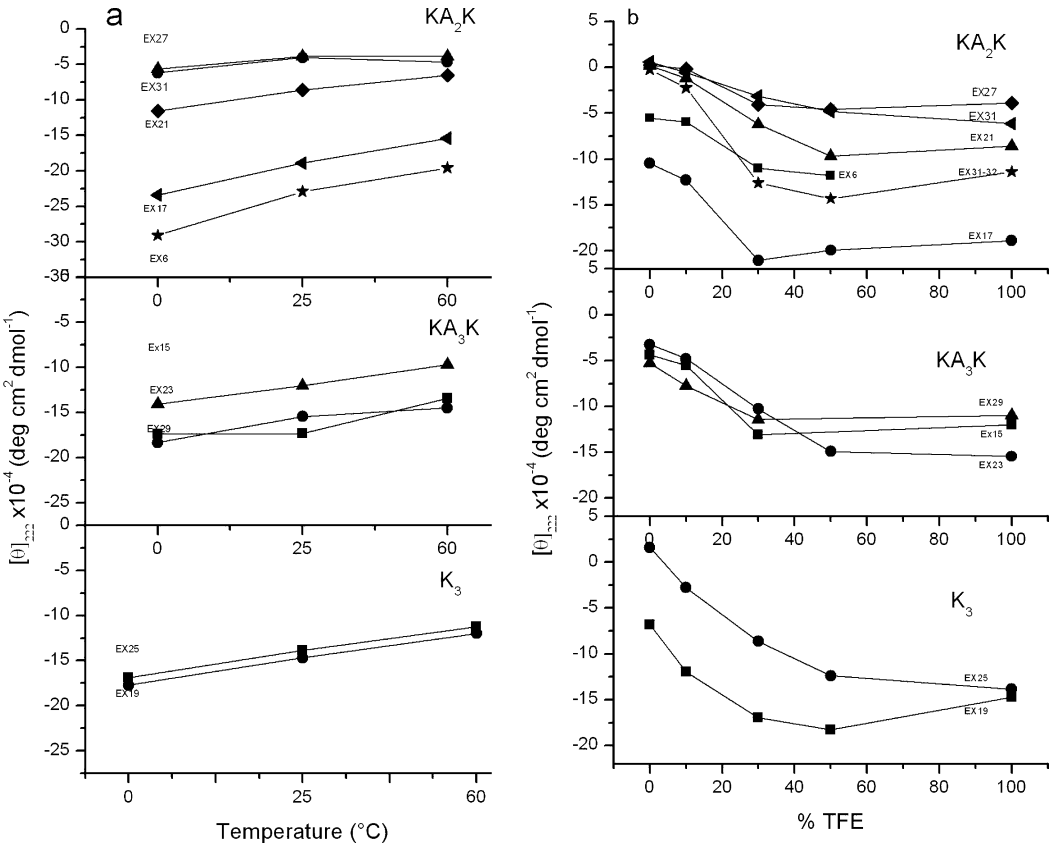

FIGURE 12: Plots reporting the stability of α-helices. $[\theta]_{222}$ as a function of temperature (a) and of TFE percentage (b).

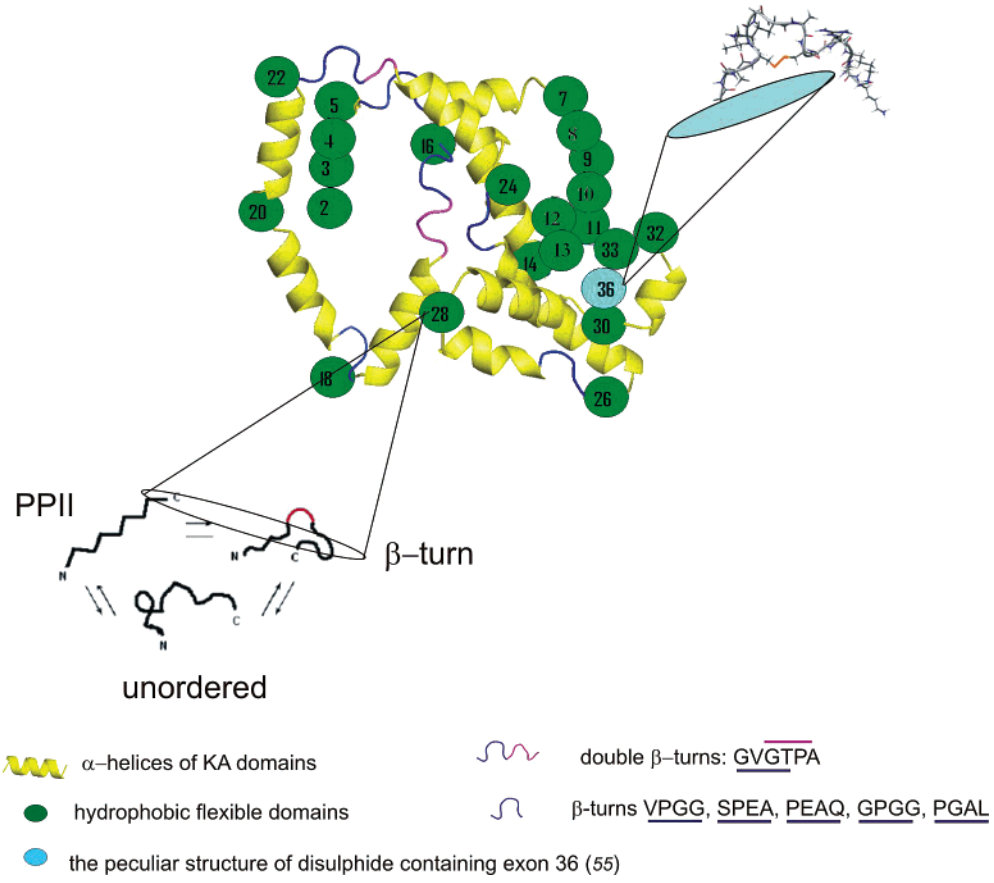

FIGURE 13: An idealized model for human tropoelastin structure.

stretch of α-helix (VRRSL), although on the C-terminal side (*51*).

(iii) The prediction algorithms, extended to the entire protein, showed the helices to be generally about the same as found by NMR. The only relevant difference appears to be an extension of the helices by some (one, two, or three, respectively) residues at the C-terminus. This apparent slight disagreement is easily explained by the disordering effect due to the C-terminal charge.

Taken together with previous results (*4*, *26*, *52*−*55*) the findings of the present paper give a complete picture of the main conformational features of human tropoelastin. We would like to emphasize that the process we accomplished of dissection and the reassembly, at both molecular and supramolecular levels, of the elastin macromolecule ("reductionist approach") has been based on the following:

(i) The gene structure of tropoelastin, a "cassette-like" organization exhibiting an almost perfect alternance between cross-linking and non-cross-linking exons, clearly argues in favor of autonomous function, and then also autonomous structures of the exons.

(ii) The extensive amount of repeating sequences present in elastin are obviously responsible for repeating structural patterns. Accordingly, even simple "monomers" or "dimers" of longer stretches (i.e., the repeating "polymers") are quite significant in terms of the overall structure.

As a matter of fact, one can envisage the whole structure of human tropoelastin as composed of 10 rather stable and essentially rigid structures, spanning a minimum of 7 and a maximum of 17 residues (see Table 2) originating the α-helical domains. These sequences are represented as helices in Figure 13. In addition, there are 5 KP domains, more flexible than the previous ones because of the presence in equilibrium of extended (PPII) and folded (type I and type II β-turns) structures (*4*). These domains comprise 90 residues and are also involved in cross-link formation mainly of the lysinonorleucine type (*25*, *27*). Therefore, flexibility should probably be specific to tropoelastin because it should significantly decrease in mature elastin after the cross-link formation.

Accordingly, 113 to 139 residues (according to either NMR or prediction algorithms) belonging to the α-helices of KA exons plus 90 belonging to KP exons of human elastin are functionally dedicated to the maintenance of the integrity of the elastomeric protein when a force is applied. The remaining residues, coded by 18 exons and comprising 483 almost hydrophobic residues plus the ones coded by cross-linking exons, but not involved in α-helices (spanning 48 to 74 residues), are responsible for the elasticity of elastin. They are characterized by multiple extended-folded equilibria in the high entropy relaxed state (*4*, *26*) whose motions have been carefully determined as chaotic, fractionary Brownian motions (*52*). A peculiar sequence is that encoded by EX36 which contains the RKRK motif, hydrophilic and highly conserved, and the two cysteine residues present in the protein which give rise to a disulfide bridge. The structure of EX36 was previously studied (*55*), and the assessed conformation is reported as a zoom image of a sky blue spheroid in Figure 13.

It has to be underlined that the size and the dimensional ratios of the figure elements (helices and spheroids) are not the real ones. Therefore, the figure has not at all to be considered as dominated by α-helices, but as an idealized, nevertheless comprehensive, model of the elastin structure.

As far as the mechanism of elastin elasticity is concerned, the picture would be the following: when the stretching force is applied, alignment of the chains occurs together with a shift of the conformational equilibria toward the extended structures with a significant decrease of both Boltzmann and (dynamic) Kolmogorov entropies. Quasi-periodic, solitonic motions are characteristic of this stretched state (*1*, *52*). After removal of the stretching force, an entropic elastic recoil should occur according to the classical theory of elasticity (*56*).

SUPPORTING INFORMATION AVAILABLE

Tables of NMR data. This material is available free of charge via the Internet at http://pubs.acs.org.

REFERENCES

1. Debelle, L., and Tamburro, A. M. (1999) Elastin: molecular description and function, *Int. J. Biochem. Cell Biol. 31*, 261−272.
2. Gibson, M. A., Hatzinikolas, G., Kumaratilake, J. S., Sandberg, L. B., Nicholl, J. K., Sutherland, G. R., and Cleary, E. G. (1996) Further characterization of proteins associated with elastic fiber microfibrils including the molecular cloning of MAGP-2 (MP25), *J. Biol. Chem. 271*, 1096−1103.
3. Gosline, J. M. (1987) Structure and mechanical properties of rubberlike proteins in animals, *Rubber Chem. Technol. 60*, 417−438.
4. Tamburro, A. M., Bochicchio, B., and Pepe, A. (2003) The dissection of Human Tropoelastin: exon by exon synthesis and related conformational studies, *Biochemistry 42*, 13147−13162.
5. Tatham, A. S., and Shewry, P. R. (2000) Elastomeric proteins: biological roles structures and mechanisms, *Trends Biochem. Sci. 25*, 567−571.
6. Bochicchio, B., Jimenez-Oronoz, F., Pepe, A., Blanco, M., Sandberg, L., and Tamburro, A. M. (2005) Synthesis of and Structural Studies on Repeating Sequences of Abductin, *Macromo. Biosci. 5*, 502−511.
7. Sandberg, L. B., Weissman, N., and Gray, W. R. (1971) Structural features of tropoelastin related to the sites of cross-links in aortic elastin, *Biochemistry 10*, 52−56.
8. Sandberg, L. B., Gray, W. R., and Bruenger, E. (1972) Structural studies of alanine- and lysine-rich regions of porcine aortic tropoelastin, *Biochim. Biophys. Acta 285*, 453−458.
9. Foster, J. A., Rubin, L., Kagan, H. M., and Franzblau, C. (1974) Isolation and characterization of cross-linked peptides from elastin, *J. Biol. Chem. 249*, 6191−6196.
10. Lent, R. W., Smith, B., Salcedo, L. L., Faris, B., and Franzblau, C. (1969) Studies on the reduction of elastin. II. Evidence for the presence of alpha-aminoadipic acid delta-semialdehyde and its aldol condensation product, *Biochemistry 8*, 2837−2845.
11. Partdridge, S. M., Eldsen, D. F., and Thomas, J. (1963) Constitution of the cross-linkages in elastin, *Nature 197*, 1297−1298.
12. Thomas, J., Eldsen, D. F., and Partdridge, S. M. (1963) Partial structure of two major degradation products from the cross-linkages in elastin, *Nature 200*, 651−652.
13. Pax, M. A., Pereyra, B., Gallop, P. M., and Seifter, S. (1974) Isomers of desmosine and isodesmosine and related reduced compounds in elastin, *J. Mechanochem. Cell Motil. 2*, 231−239.
14. Piez, K. A. (1968) Cross-linking of collagen and elastin, *Annu. Rev. Biochem. 37*, 547−570.
15. Gray, W. R., Sandberg, L. B., and Foster, J. A. (1973) Molecular model for elastin structure and function, *Nature 246*, 461−466.
16. Foster, J. A., Bruenger, E., Rubin, L., Imbermin, M., Kagan, H., Mecham, R. P., and Franzblau, C. (1976) Circular dichroism studies of an elastin crosslinked peptide, *Biopolymers 15*, 833−841.
17. Vrhovski, B., Jensen, S., and Weiss, A. S. (1997) Coacervation characteristics of recombinant human tropoelastin, *Eur. J. Biochem. 250*, 92−98.

18. Muiznieks, L. D., Jensen, S. A., and Weiss, A. S. (2003) Structural changes and facilitated association of tropoelastin, *Arch. Biochem. Biophys. 410*, 317−323.
19. Debelle, L., Alix, A. J. P., Jacob, M. P., Huvenne, J. P., Berjot, M., Sombret, B., and Legrand, P. (1995) Bovine elastin and kappa-elastin secondary structure determination by optical spectroscopies, *J. Biol. Chem. 270*, 26099−26103.
20. Miao, M., Cirulis, J. T., Lee, S., and Keeley, F. W. (2005) Structural determinants of cross-linking and hydrophobic domains for self-assembly of elastin-like polypeptides, *Biochemistry 44*, 14367−14375.
21. Wender, D. B., Treiber, L. R., Bensusan, H. B., and Walton, A. G. (1974) Synthesis and characterization of poly($LysAla_3$), *Biopolymers 13*, 1929−1941.
22. Mecham, R. P., and Foster, J. A. (1978) A structural model for desmosine cross-linked peptides, *Biochem. J. 173*, 617−625.
23. Bashir, M. M., Indik, Z., Yeh, H., Ornstein-Goldstein. N., Rosenbloom, J. C., Abrams, W., Fazio, M., Uitto, J., and Rosenbloom, J. (1989) Characterization of the complete human elastin gene. Delineation of unusual features in the 5′-flanking region, *J. Biol. Chem. 264*, 8887−8891.
24. Yeh, H., Anderson, N., Ornstein-Goldstein, N., Bashir, M. M., Rosenbloom J. C., Abrams, W., Indik, Z., Yoon, K., Parks, W., and Mecham, R. P. (1989) Structure of the bovine elastin gene and S1 nuclease analysis of alternative splicing of elastin mRNA in the bovine nuchal ligament, *Biochemistry 28*, 2365−2370.
25. Brown-Ausburger, P., Tisdale, C., Broekelmann, T., Sloan, C., and Mecham, R. P. (1995) Identification of an elastin cross-linking domain that joins three peptide chains. Possible role in nucleated assembly, *J. Biol. Chem. 270*, 17778−17783.
26. Bochicchio, B., Pepe, A., and Tamburro, A. M. (2005) The dissection of human tropoelastin: from the molecular structure to the self-assembly to the elasticity mechanism, *Pathol. Biol. 53*, 383−389.
27. Wise, S. G., Mithieux, S. M., Raftery, M. J., and Weiss, A. S. (2005) Specificity in the coacervation of tropoelastin: solvent exposed lysines, *J. Struct. Biol. 149*, 273−281.
28. Garnier, J., Gibrat, J. F., and Robson, B. (1996) GOR method for predicting protein secondary structure from amino acid sequence, *Methods Enzymol. 266*, 540−553.
29. Combet, C., Blanchet, C., Geourjon, C., and Deléage, G. (2000) NPS@: network protein sequence analysis, *Trends Biochem. Sci. 25*, 147−150.
30. Garnier, J., Osguthorpe, D., and Robson, B. (1978) Analysis of the accuracy and implications of simple methods for predicting the secondary structure of globular proteins, *J. Mol. Biol. 120*, 97−120.
31. Kneller, D. G., Cohen, F. E., and Langridge, R. (1990) Improvements in protein secondary structure prediction by an enhanced neural network, *J. Mol. Biol. 214*, 171−182.
32. Baldi, P., and Pollastri, G. (2003) The principled design of large-scale recursive neural network architectures-DAG-RNNs and the protein structure prediction problem, *J. Machine Learning Res. 4*, 575−603.
33. Wüthrich, K. (1986) *NMR of Proteins and Nucleic Acids*, Wiley, New York.
34. Davis, D. G., and Bax, A. (1985) MLEV-17-based two-dimensional homonuclear magnetization transfer spectroscopy, *J. Am. Chem. Soc. 107*, 2820−2821.
35. Jeener, J., Meier, B. H., Bachmann, P., and Ernst, R. R. (1979) Investigation of exchange processes by two-dimensional NMR spectroscopy, *J. Chem. Phys. 71*, 4546−4553.
36. Wüthrich, K., Billeter, M., and Braun, W. (1983) Pseudo-structures for the 20 common amino acids for use in studies of protein conformations by measurements of intramolecular proton-proton distance constraints with nuclear magnetic resonance, *J. Mol. Biol. 169*, 949−961.
37. Guntert, P., Mumenthaler, M., and Wüthrich, K. (1997) Torsion angle dynamics for NMR structure calculation with the new program DYANA, *J. Mol. Biol. 273*, 283−298.
38. Koradi, R., Billeter, M., and Wüthrich, K. (1996) MOLMOL: a program for display and analysis of macromolecular structures, *J. Mol. Graph 14*, 51−55.
39. Indik, Z., Yeh, H., Ornstein-Goldstein, N., Sheppard, P., Anderson, N., Rosenbloom, J. C., Peltonen, L., and Rosenbloom, J. (1987) Alternative splicing of human elastin mRNA indicated by sequence analysis of cloned genomic and complementary DNA, *Proc. Natl. Acad. Sci. U.S.A. 84*, 5680−5604.
40. Bodkin, M. J., and Goodfellow, J. M. (1996) Hydrophobic solvation in aqueous trifluoroethanol solution, *Biopolymers 39*, 43−50.
41. Buck, M. (1998) Trifluoroethanol and colleagues: cosolvents come of age. Recent studies with peptides and proteins, *Q. Rev. Biophys. 31*, 297−355.
42. Reiersen, H., and Rees, A. R. (2000) Trifluoroethanol may form a solvent matrix for assisted hydrophobic interactions between peptide side chains, *Protein Eng. 13*, 739−743.
43. Scatturin, A., Tamburro, A. M., Rocchi, R., and Scoffone, E. (1967) The conformation of bovine pancreatic ribonuclease S-peptide, *Chem. Commun.* 1273−1274.
44. Tamburro, A. M., Scatturin, A., Rocchi, R., Marchiori, F., Borin, G., and Scoffone, E. (1968) Conformational-transitions of bovine pancreatic ribonuclease S-peptide, *FEBS Lett. 1*, 298−300.
45. Wyckoff, H. W., Hardman, K. D., Allewell, N. M., Inagami, T., Johnson, L. N., and Richards, F. M. (1967) The structure of ribonuclease-S at 3.5 Å resolution, *J. Biol. Chem. 242*, 3984−3948.
46. Wishart, D. S., Sykes, B. D., and Richards, F. M. (1992) The chemical shift index: a fast and simple method for the assignment of protein secondary structure through NMR spectroscopy, *Biochemistry 31*, 1647−1651.
47. Bochicchio, B., and Tamburro, A. M. (2002) Polyproline II structure in proteins: identification by chiroptical spectroscopies, stability, and functions, *Chirality 14*, 782−792.
48. Woody, R. W. (1992) Circular dichroism and conformation of unordered polypeptides, *Adv. Biophys. Chem. 2*, 37−39.
49. Venugopal, M. G., Ramshaw, J. A., Braswell, E., Zhu, D., and Brodsky, B. (1994) Electrostatic interactions in collagen-like triple-helical peptides, *Biochemistry 33*, 7948−7956.
50. Bochicchio, B., Floquet, N., Pepe, A., Alix, A. J. P., and Tamburro, A. M. (2004) Dissection of human tropoelastin: solution structure, dynamics and self-assembly of the exon 5 peptide, *Chem. Eur. J. 10*, 3166−3176.
51. Bisaccia, F., Castiglione-Morelli, M. A., Spisani, S., Serafini-Fracassini, A., and Tamburro, A. M. (2000) Solution structure of the amino acid sequence coded by the rarely expressed exon 26A of human elastin: the N-terminal region, *J. Pept. Res. 56*, 201−209.
52. Villani, V., Tamburro, A. M., and Zaldivar Comenges, J. (2000) Conformational chaos and biomolecular instability in aqueous solution, *J. Chem. Soc., Perkin Trans. 2*, 2177−2184.
53. Pepe, A., Guerra, D., Bochicchio, B., Quaglino, D., Gheduzzi, D., Pasquali Ronchetti, I., and Tamburro, A. M. (2005) Dissection of human tropoelastin: supramolecular organization of polypeptide sequences coded by particular exons, *Matrix Biol. 24*, 96−109.
54. Tamburro, A. M., De Stradis, A., and D'Alessio, L. (1995) Fractal aspects of elastin supramolecular organization, *J. Biomol. Struct. Dyn. 12*, 1161−1172.
55. Floquet, N., Pepe, A., Dauchez, M., Bochicchio, B., Tamburro, A. M., and Alix, A. J. P. (2005) Structure and modeling studies of the carboxy-terminus region of human tropoelastin, *Matrix Biol. 24*, 271−282.
56. Flory, J. (1953) *Principles of polymer chemistry*, Ithaca, NY, Cornell University Press.

BI060289I